Circularly Polarized Retrodirective Antenna Array for Wireless Power Transmission

Circularly Polarized Retrodirective Antenna Array for Wireless Power Transmission

P. D. Hilario Re, *Student Member IEEE*, S. K. Podilchak, *Member IEEE*, S. Rotenberg, *Student Member IEEE*, G. Goussetis *Senior Member, IEEE* and J. Lee

***Abstract*—A retrodirective antenna (RDA) array for wireless power transmission (WPT) is presented. Applications include the wireless charging of mobile phones and other handheld devices. The reported RDA defines an active high-power transmitter module which retrodirects a received beacon tone back to a mobile unit by circularly polarized (CP) free-space radiation. In addition, this RDA architecture uses a network of 4 sub-arrays, defined by a total of 16 radiating patch elements, in an effort to boost the transmit gain while also reducing the supporting RF hardware requirements when compared to a more conventional RDA. Measurements and simulations in the reactive near-field of the system are in agreement in terms of the tracking capabilities of the high-power CP-RDA. Power levels in excess of 27 dBm were measured at 2.4 GHz at a receiver module, and when this RF power was rectified, more than 350 mW at DC was observed. To the best knowledge of the authors, this is the first demonstration of a WPT system using a mixer-based analog-RDA. Previous low power demonstrations were more complex computer-controlled systems which did not offer any real-time tracking ability. Other applications for the proposed RDA include target tracking, sensor charging, and other WPT systems.**

***Index Terms*—Arrays, heterodyning, planar arrays, retrodirective antennas, retrodirectivity.**

I. Introduction

Cutting the last wire between the power source and the device-under-charge (DUC) with flexible mobility and efficient power transfer is the main aim of wireless power transmission (WPT). This ever advancing technology can be formally defined as the transmission of power from a source to a receiving device without any physical connection between them. Such a concept is illustrated in Fig. 1, where we can differentiate between a wireless charger in the reactive near-field (NF) and a charger operating in either the reactive NF, the radiative NF, or the far-field (FF). WPT systems can be further classified based on the operating frequency where microwave power transfer (MPT) relates to WPT systems that work at these frequencies, being the focus of this paper. Some previous MPT research has also been reported for solar power harvesting and the remote powering of unmanned aerial vehicles [1]–[3].

The first of the WPT systems shown in Fig. 1(a) is based on resonant inductive coupling between two coils that are designed to resonate at the same frequency [4]–[7]. In order to achieve efficient transfer of power, both transmit and receive coils must be in the reactive NF region and properly aligned [8]. This limits the positioning of the DUC to be at an extremely short distance with respect to the transmitter for efficient power transfer. Some applications of this type of NF-WPT system have been applied to the wireless charging of consumer electronics [4], [5], electrical vehicles [6], and biomedical devices [7].

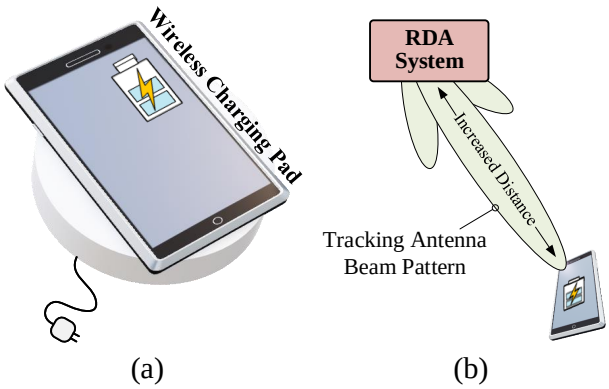

Fig. 1. Conventional WPT by inductive coupling (a), and the proposed WPT approach using retrodirective antenna (RDA) technology (b) where the device can be tracked and its battery charged in free-space at an increased distance.

The limitations, in terms of the distance and positioning of the charging pad and DUC for this type of WPT (Fig. 1(a)) can be overcome by radiating WPT systems (Fig. 1(b)). This system permits the DUC to move freely at considerable distances from the charger when compared to the first approach. However, more power loss can be observed in the transmission path due to free-space path losses (FSPLs) for the radiating WPT system. Even though these losses can be partially compensated by the use of high gain antennas, the resulting directive beam patterns can lead to alignment requirements, but at the same time, increased levels of received power at the DUC.

One technology that can be adopted for this radiating WPT antenna system, as in our proposed work and in an effort to circumvent these problems, is a type of self-steering, or tracking retrodirective antenna (RDA) array where the beam pattern maximum for the transmitter is directed towards the receiver. In particular, one of the main advantages when considering RDAs for WPT is the near-field-focused beamforming that they can provide which is mainly due to the phase conjugation of an incoming beacon signal incident onto a receiver array, and then, re-radiation back to the DUC, as in the adopted scenario. This is important for WPT systems since a power focal point can be constructed at the location of the DUC since the contributions of the individual transmitter RDA elements can be summed in phase.

It should also be mentioned that some other works have

applied different beam-steering technologies, and with the noted WPT application in mind. For example, in [9], a tracking system was shown using digital beam forming, while in [10], an RDA was also used as a transmitter. That work focused on how to optimize the number of receiver rectennas and how to maximize the overall efficiency. In both of these papers, no complete antenna system results were reported. In addition, RDAs have been developed for other applications including spatial encryption, radar, and microwave imaging [11]. Given that RDAs can operate either in the NF [12], [13] or in the FF [11], [14], there can be some considerable advantages over the traditional reactive NF wireless chargers while also providing more convenience for the user.

In a classical two-dimensional (2-D) $M \times N$ RDA, for example, which operates by heterodyne mixing (a Pon structure [15]), every antenna element is typically associated with an individual mixer, an amplifier, and a circulator (see Fig. 2(b)). This enables 2-D self-steering in the $\hat{\theta}$ and $\hat{\phi}$ directions; i.e. the retrodirected power is related to the steered realized gain pattern, $|G(\theta, \phi)|$, due to an incoming beacon signal. If we take into account the number of supporting RF circuit components, the costs can increase, especially when considering WPT in that a significant number of radiating elements and high power amplifiers are required to circumvent the aforementioned FSPLs.

In order to reduce these associated implementation costs, while maintaining the highest possible received power levels at the DUC when compared to a system which uses a more conventional Pon RDA (Fig. 2(a)), an alternative architecture is proposed in this work. In particular, we design and measure a novel CP-RDA for WPT applications by exploiting sub-arrays at transmit (see Fig. 2(c)), mainly to simplify and reduce the number of active components needed for the RDA and therefore minimizing costs. For example, circulators are not required for our proposed RDA due to having independent transmit and receive antennas, and amplifier-mixer pairs are not needed at each radiating element. This comes at a cost of NF focusing in one plane only and reduced scanning capability in the $\phi = 90^\circ$ plane when considering the FF; i.e. the retrodirected pattern is defined by $G(\theta)$ only (and not $G(\theta, \phi)$ when compared to the conventional 2-D RDA). Regardless of this trade-off, it will be shown in the paper that self-steering is still effective for the proposed WPT application while also offering reduced implementation costs.

To the best of our knowledge no similar demonstration of WPT using an analogue mixer-based RDA for received power levels as high as 350 mW and based on an adapted version of the classic Pon RDA, has not been reported in the literature previously. In particular, the proposed RDA demonstrates a transmitted output power of 36 dBm by retrodirecting and amplifying the received beacon tone which was generated by a voltage controlled oscillator (VCO) with a power level of 6.6 dBm. Moreover, when considering operation for the proposed WPT system, we define the proposed RDA as the transmitter module. When this retrodirected RF power is received in the reactive NF and rectified at the DUC (defined as the receiver module considering $50\,\mathrm{cm}$ of radial separation between the RDA and DUC in our antenna system), more than $350\,\mathrm{mW}$ were measured at DC using the rectifier reported in [16] which had demonstrated RF-to-DC efficiency values of more than 75%.

The paper is organized as follows. In section II, an overview of different RDA architectures is discussed and a cost comparison study is reported where an alternative design is developed which uses sub-arrays. Details of the proposed RDA architecture are also given. Section III discusses the simulations and measurements of this RDA and its operation within a WPT system while a comparison is made with other relevant structures found in the literature. To conclude, Section IV summarizes the important findings of the present work.

II. RDA Design Overview Considering WPT

Classic RDAs can be defined as an array of transceivers that are able to self-track objects by conjugating the relative phase difference received at each antenna element [17]. These antenna systems require a large number of radiating elements when considering WPT applications; for example, when charging remote mobile phone batteries in the FF. In addition, high gain RF amplifiers are of vital importance to boost the power delivery to the DUC.

A. RDA Architecture Selection and Design

RDAs can be divided into two main subgroups: Pon [15] and Van Atta [18] structures. Passive Van Atta structures are defined by an even number of antennas connecting one antenna to its symmetric pair with respect to the phase centre of the array and introducing a phase delay of 180° between them whilst typically using transmission line connections. Active Van Atta RDAs generally also require a supporting circuit arrangement of amplifiers and circulators, or just bi-directional amplifiers [19] which can make the structure high-cost for implementation in an antenna system for WPT.

On the other hand, Pon architectures provide retrodirectivity by phase conjugation using RF mixers [11] where an $M \times N$ schematic is shown in Fig. 2(b). The underlying principle of phase conjugation for the Pon structure [15] can be further understood by studying the product of two cosines, defined at the input RF of a mixer and the local oscillator signal (LO). In the literature, spherical [20] and cylindrical [21] Pon RDA structures have also been reported, but planar and more low profile architectures may be preferred for consumer electronics and WPT applications.

When the beacon signal for tracking is sent by the DUC and received at the RDA, it gets mixed at each RF mixer (heterodyning) which share a common LO, enabling phase conjugation of the output [15]. In particular, this phase conjugation will induce an inverted progressive phase difference between consecutive array elements, resulting in a wave-front with the same direction as the received one. As this phenomena happens in real-time for an analog-based antenna system, beam tracking of the DUC is therefore based on the incoming beacon signal.

Some practical challenges can also come about when selecting the transceiver design frequencies for the RDA and when employing circulators to isolate the signals with conventional

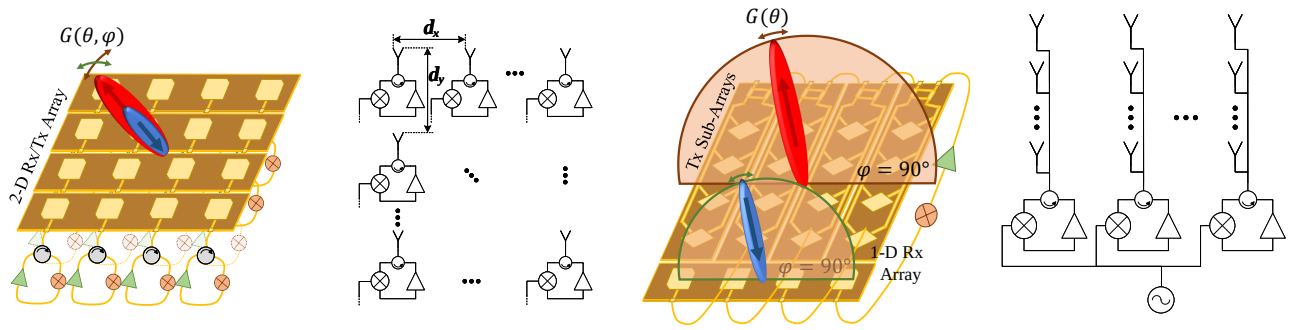

(a) (b) (c) (d)

Fig. 2. Comparison of a more conventional CP-RDA (a-b), defined by a 2-D planar array of corner-clipped patches and heterodyne mixing (i.e. a Pon architecture where RF amplifiers, circulators and mixers are required at each antenna element, as in (b)) to the proposed RDA (c-d). In both cases, a total of 16-elements (4×4) are illustrated for the transmitting part of the RDA.

RDAs. For example, typical isolation values between non-consecutive ports are from 20 to 40 dB for off-the-shelf circulator components. When considering high-power WPT applications, as in this work, an unwanted feedback loop (for the high-power re-transmitted signal) can potentially be induced due to circulator leakage causing unwanted mixing within the RF chain and parasitic radiation. This can also overload some active components and cause permanent damage to high gain amplifiers. In addition, circulators are typically bulky and expensive, making them not a preferred option when considering low-profile and low-cost WPT system implementation for consumer electronics.

B. Cost Considerations and Maintained Performance

When considering RDAs, self-steering in 3-D space or within two distinct angular directions is generally more preferred. This is because the re-radiated gain pattern can be steered in the $\hat{\theta}$ and $\hat{\phi}$ directions which typically requires a 2-D array (see Fig. 2(a-b)). The cost for this type of Pon RDA architecture can increase significantly due to the number of antenna elements as well as the supporting RF circuit hardware (see Table I).

This is where the benefits of the proposed RDA can be further appreciated. In this work, we are seeking a compromise between 2-D self-tracking performance, received power at the DUC, and overall antenna system implementation cost. This is because it can be expected that the majority of the costs in a 2-D RDA system (see Fig. 2(b)) are related to the number of active devices (i.e. mixers, amplifiers, etc.), perhaps making RDA development challenging for WPT applications when self-tracking in two angular directions is required.

To circumvent these issues, the proposed RDA architecture is a hybridization between 1-D and 2-D arrays. This concept is further illustrated in Fig. 2(c-d) where a network of sub-array elements are employed instead of one radiating element for each RF mixer-amplifier pair as in a more conventional 2-D RDA. It should be mentioned that the proposed RDA, can be considered more as a 1-D RDA since tracking is only in the y-z ($\phi = 90°$) plane with a steered re-radiated pattern defined by $G(\theta)$. At the same time our proposed RDA, with 16 ($= 4\times4$) radiating elements, can reduce the costs by almost 2 times when compared to a more standard 2×4, 2-D RDA whilst offering similar power levels. This is further examined in Table I. This single-plane scanning, may be appropriate because of its minimal reduction of received power when the DUC is within the main tracking plane and near broadside.

The impact of this power loss (when away for the main tracking plane) is further examined in Fig. 3 where the scanning of a 1-D array is compared to that of a 2-D array. Moreover, the aim of the study in Fig. 3 is to compare the simulated power loss of the proposed design to that of a full 2-D RDA along the $\phi = 90°$ plane. This comparison is also illustrated in Figs. 2(a) and (c) for the RDA architectures. It should also be mentioned that for both cases, the dimensions of the transmitting arrays are 4×4, employing CP patches that operate at the working frequency and are spaced $\lambda_0/2$.

In Fig. 3, the red solid line represents the normalized gain of the transmitting array for the proposed RDA, in the FF, for each position of the DUC from 0° to 90° along the non-tracking plane ($\phi = 0°$). As it can be seen, the normalized pattern will stay fixed with its maxima pointing at broadside. Conversely, for the comparative 4×4 2-D RDA, tracking is still observed in that plane as it is shown in the solid blue line since power levels for 2-D tracking systems are higher than that of the 1-D one. This solid blue line represents all the maximums of each of the patterns that would be generated by the full 2-D RDA in the FF. Also, some of the individual FF patterns are also shown in Fig. 3 (dashed gray lines).

The difference between the two traces, represents the power drop in the non-tracking plane for the proposed RDA in comparison to that of a more conventional 4×4 2-D RDA. From this comparison, depending on how critical the loss of power is, in terms of cost and the application, the proposed RDA may be favored when compared to a 2-D RDA. This is because the proposed RDA maintains consistent values at angles close to broadside. Also, power degradations of only about 5 dB are observed from broadside to $\theta = 30°$. In terms of cost, the more conventional 2-D RDA exhibits full tracking capability and higher received power, but is almost 4 times the cost of the proposed design. This comparison is further described in Table I.

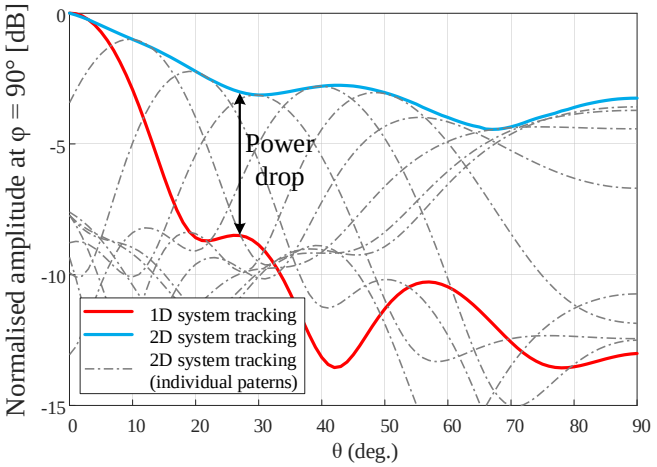

Fig. 3. Tracking power loss comparison when away from the dominant steering plane (which is defined at $\phi = 90°$). Reduced power values of only about 5 dB are observed from broadside to $\theta = 30°$ in the FF for the simulated 1-D tracking system (which is representative of the proposed RDA defined by linear 1-D sub-array elements) when compared to a more conventional 2-D RDA. It should also be mentioned that for both 1-D and 2-D architectures, 16 radiating elements in total were simulated for a fair comparison.

TABLE I
RECEIVED RF POWER AND COST VERSUS RDA SIZE

RDA Array Size (IN / OUT)[1]	Normalized Performance[2]	Normalized Cost[3]
2×1 / 2×1	1	1
2×2 / 2×2	4.4	1.9
2×3 / 2×3	9.7	2.7
2×4 / 2×4	17.1	3.5
4×4 / 4×4	66.7	6.9
Proposed work (4×1 / 4×4)	16.7	1.8

[1] *Array Size* corresponds to the size of the separated receiving and transmitting arrays of the RDA given that this comparison is made for RDAs that do not use circulators as shown in Fig. 2(c-d), where IN/OUT refers to size of the input receive and output transmit antenna array for the RDA operating at 2.5 GHz and 2.4 GHz, respectively. The reported values in these performance and cost estimations were also obtained by considering the simulated realized gain of an individual patch antenna, employed in the proposed design, computed with the array factor for a $\lambda/2$ separation between elements.

[2] *Normalized Performance* corresponds to the received RF power at the DUC for a 0.5 m distance between the RDA and the DUC, and normalized, with respect the 2×1 (IN and OUT) RDA. It should also be mentioned that *Normalized Performance* = 15, which is our design goal, and corresponds to 27 dBm. Moreover, the gains and losses of the active RF devices to compute the overall performance for each of the cases was obtained from the datasheets of the employed circuit components (see Fig. 4).

[3] *Normalized Cost* refers to the total cost of the active components needed for each case and normalized with respect the 2×1 (IN and OUT) RDA.

C. Design of the Proposed RDA

The design under study is shown in Fig. 2(c) and the measured prototype is shown in Fig. 4. It comprises a 4×1 input and a 16-element output array which is subdivided into 4 distinct sub-arrays (of size 4×1) on each RF chain. In terms of polarisation, the system exhibits RHCP in the 4×1 receiver array and LHCP in the 16-element transmitter array so that there is isolation between the two arrays and orientation flexibility in the positioning of the DUC which brings high levels of mobility when considering the intended application of mobile phone charging.

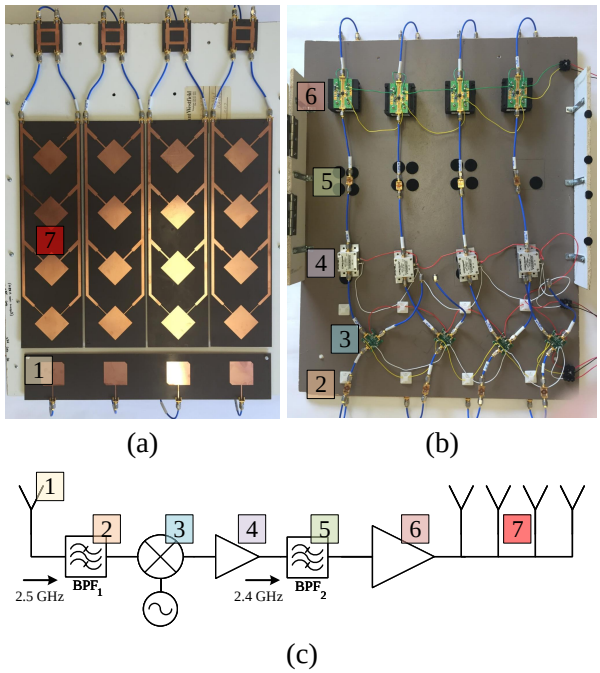

Fig. 4. Picture of the developed RDA system. Front (a), back (b) and schematic of one of the four RF chains (c). The components used in the antenna system for each RF chain: (1) 2.5 GHz RHCP corner clipped patch (part of the 4×1 receiver array), (2) band pass filter from TriQuint 885009 at 2.5 GHz, (3) mixer from Linear Technology LTC5549, (4) driver amplifier from MiniCircuits ZFL-2500+, (5) band pass filter from TriQuint 885017 at 2.4 GHz, (6) power amplifier from TriQuint TQP9111 and (7) 2.4 GHz LHCP 4×1 sub-array (part of the 16 element transmitter array).

The input RF signal to be mixed is chosen to be 2.5 GHz, the LO frequency is 4.9 GHz, and therefore the IF frequency is 2.4 GHz requiring the selection of downconverting mixers. At the output of the mixers, amplifiers are also required in order to achieve high power levels at the DUC. This makes the RF chain require a driver and a power amplifier, the latter being in saturation.

As circulators are not used, the antenna system still needs to aim for minimum electromagnetic coupling between transmit and receive arrays. This is important for the intended high power application and for correct RDA operation. The fact that both antennas are working at similar frequencies (2.5 GHz for the 4×1 receive and 2.4 GHz for the 4×4 transmit) and within close proximity, any coupling still needs to be minimized for optimal system performance. This required the use of a bandpass filter (BPF_1) immediately after the receiving antennas within the RF chain, which exhibited an out of band rejection of -36.8 dB. This avoids any unwanted feedback loop between the transmitter and the receiver of the RDA.

At the input RF port of the mixers some of the input 2.5 GHz signal can leak through the mixers, get re-amplified, re-transmitted, and then coupled back and combined with the original 2.5 GHz received signal. This can slightly mask the phase difference to be conjugated at the receiver array elements and can possibly lead to a beam pointing error upon re-radiation. To minimize this issue, a second BPF (BPF_2) was introduced in the RF chain right after the driver amplifier

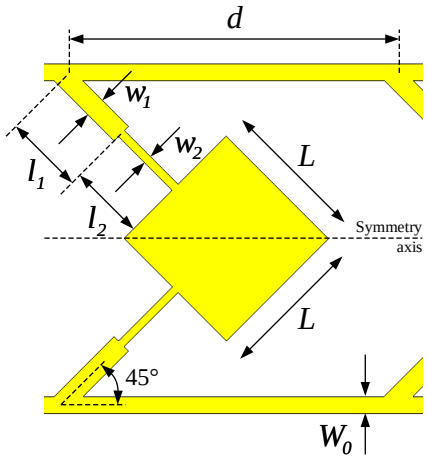

Fig. 5. Schematic of the antenna element within the 2.4 GHz LHCP transmit array (see Fig. 4(a)).

that will allow the transmitting signal to pass through and reject any unwanted signal leaked from the mixer. In this case, an out of band rejection of -31 dB was achieved. Some simulations where also completed prior to fabrication to quantify the electromagnetic coupling between the transmit and receive antenna arrays for both frequencies. These simulations were defined by just the passive antenna array elements within the transmitter module. The coupling was below -45 dB and -40 dB at 2.4 GHz and 2.5 GHz, respectively. Given these values as well as the aforementioned out of band rejection levels and the RF to IF isolation in the mixer, any coupling between the receiving and transmitting arrays for the RDA are expected to be minimal.

The final schematic for one RF chain for the proposed RDA is shown in Fig. 4(c). The transmitting and receiving arrays were fabricated using a Taconic TLY-5 substrate, with a dielectric constant ϵ_r = 2.2 and a thickness of $h = 1.57\,\mathrm{mm}$. As it is shown in Fig. 4(a), the patches of the transmitting sub-arrays are series-fed, as in [22], with a split of approximately 3 dB for each element. This defines a relative amplitude ratio distribution of about $1/2, 1/4, 1/8$ and $1/8$. This series

TABLE II
DIMENSIONS OF ONE SECTION FROM THE PROPOSED SUB-ARRAY

Dimension	Millimeters [mm]
l_1	24.22
w_1	5.74
l_2	21.4
w_2	2.32
l_2'	21.4[1]
w_2'	1.02[1]
L	40.63
W_0	4.71
d	92.75

[1] The last antenna element has different dimensions for l_2 and w_2 for better matching and termination of the sub-array. For this case, the relevant variables are l_2' and w_2'.

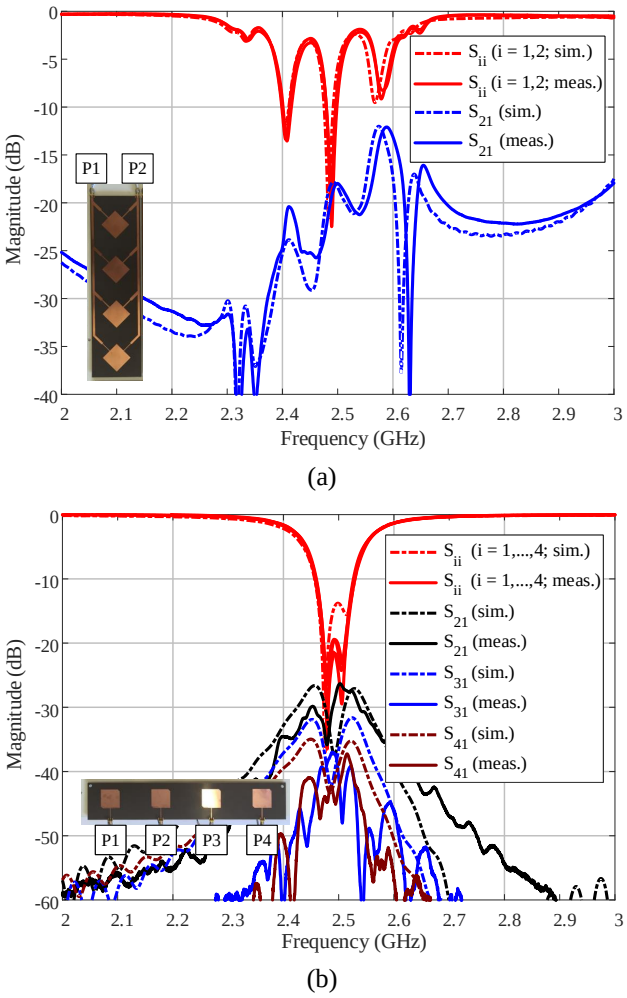

Fig. 6. S-Parameters of the 4×4 transmit (one sub-array) (a) and 4×1 receive (b) arrays within the proposed RDA for operation at 2.4 GHz and 2.5 GHz respectively.

feeding approach was employed for each sub-array mainly due to its simple design which provided suitable gain values and acceptable side lobe levels. In particular, gain values approached 19 dBic for the complete transmitter; i.e. 4 sub-arrays (see Fig. 2(c) and 4) while side-lobe levels (SLLs) were about 10 dB or below from the main beam maximum (all results not shown for brevity). Also, for good 50-Ω matching, two independent $\lambda/4$ impedance transformers were placed between the periphery feed lines and the patches. Also, the distance between consecutive patches within the sub-array is such that each one radiates in phase. More details regarding the dimensions of the elements within the sub-array can be found in Fig. 5 and Table II.

For CP radiation hybrid couplers were also employed just before the sub-arrays, which are used to apply a phase offset of 90° between the two feed lines connected to the square patches. One advantage of using the hybrid couplers is that depending on the selected input port, it is possible to make the re-radiated transmission from the RDA to be either LHCP or RHCP when polarization diversity is needed. Additionally, 50-Ω loads were connected to the isolated ports of the couplers for proper termination during antenna system integration.

Regarding the 4×1 receiver array, the corners of the patches were truncated for RHCP, simply allowing for one port per patch and defining a total of 4 RF chains (see Fig. 4) for the proposed RDA.

In Fig. 6, the S-Parameters for one of the four transmit 4×1 subarrays and the 4×1 receive array are shown, respectively. There is a good agreement between simulations and measurements, and the coupling levels between ports at the transmit frequency in Fig. 6(a) are below 20 dB. Due to the spurious feed radiation there is an unwanted minimum in the reflection coefficient at around $2.5\,\mathrm{GHz}$; i.e. $|S_{11}|$ < -10 dB which may be caused by the unbalanced dual-orthogonal feeds of the square patches [23] with some small and unwanted radiation. However, this issue is mitigated by the second BPF in the RF chain. For the receiver 4×1 array, good 50-Ω matching can be achieved at the desired 2.5 GHz receiving frequency (see Fig. 6(b)) while a high rejection at the retrodirected frequency is likely since the antenna is not well matched at $2.4\,\mathrm{GHz}$. Moreover, the coupling values between patches are below 25 dB at the $2.5\,\mathrm{GHz}$ receiving frequency.

In order to test the RDA, an initial tone at $2.5\,\mathrm{GHz}$ was generated with one transmitting reference patch antenna. This tone is received by the RDA and retrodirects the re-amplified signal at $2.4\,\mathrm{GHz}$ back towards the receiver module, which is designed using a 2×1 patch antenna array working at $2.4\,\mathrm{GHz}$ and a Wilkinson power combiner as shown in Fig. 7.

III. Results and Discussion

Regarding the measurement setup, a N9030B PXA Signal Analyser from Keysight Technologies was used to measure the received power level at the output of the Wilkinson power combiner, a N5182B MXG Vector Signal Generator from Keysight Technologies to generate the $4.9\,\mathrm{GHz}$ tone for connectivity to the LO ports of the mixers, and power supplies were used (in series) to bias the twelve RF active devices for the antenna system.

In order to test the tracking capabilities of the system, bistatic and monostatic measurements (see Fig. 7) were performed for the RDA. Measurements were carried out at a 50 cm radial distance between the RDA and receiver module, for design and system implementation purposes. It is also worth mentioning that all the measurements were completed in the reactive NF region. This is because the boundary that defines the transition into the radiative NF zone is about $75\,\mathrm{cm}$.

For the monostatic case (Fig. 7(a)), transmit and receive antennas (receiver module) move together around the RDA in order to record the retrodirected power values at each angle. However, in order to measure the radiated RDA pattern at a given angle, bistatic measurements are also needed (Fig. 7(b)). In this case, the transmit beacon is fixed at a certain angle making the RDA focus its retrodirected beam to that position. Then, the receive antenna within the receiver module is moved around the RDA on a circular arc (with a fixed range) being able to measure the re-radiated pattern from the RDA.

In Fig. 8 a comparison between the simulated and measured bistatic patterns is shown. All the patterns are normalized with respect the maxima for the broadside case. Simulations were

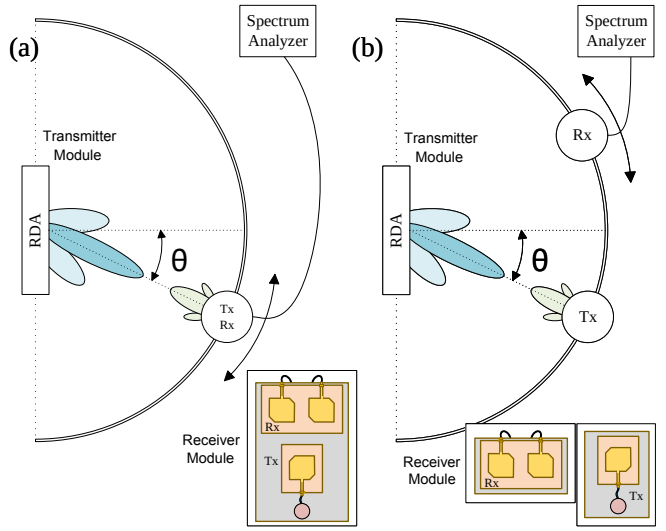

Fig. 7. Monostatic (a) and bistatic (b) measurement illustrations with the transmitter and receiver schematics shown in the inset for each case (receiver module). Also, the RDA is defined as the transmitter module.

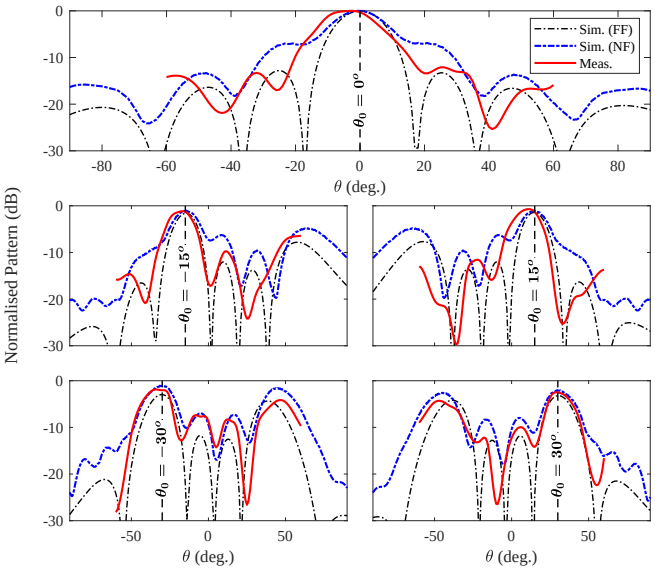

Fig. 8. Simulated (black dot-dashed and blue dashed lines) and measured (red line) normalised bistatic patterns at 2.4 GHz and sampled at the receiver module for different beacon incidence angles (from top-down and left-right: broadside, -15°, +15°, -30° and +30°). Note: the NF results were both sampled at a range of 50 cm from the RDA.

completed by applying the required relative phase difference between elements that will make the main beam point to the predefined angle. It can be observed that there is a small shift in the measured beam angle position with respect to the simulated one. This can be caused by the internal phase noise that the active components within the circuit system can generate as well as potential uneven power outputs from each amplifier. There could have also been some small mechanical misalignment during the measurement trials. Additionally, the minor differences between the measured and simulated beam patterns can be related to the fact that simulations were based on FF patterns and NF data, whereas the measured bistatic patterns were completed in the reactive NF. Regardless, results still show tracking capability for different pointing angles

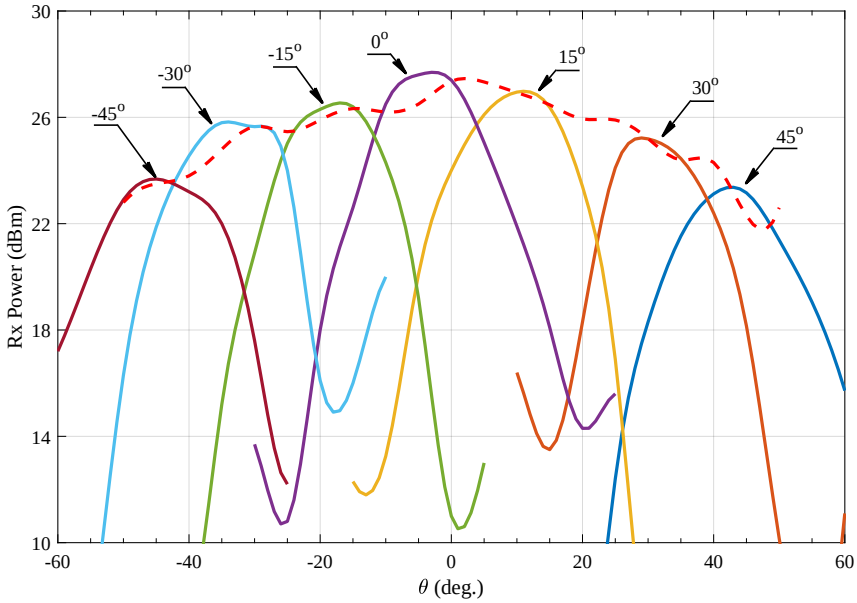

Fig. 9. Measured monostatic (dashed line) and bistatic received power (solid lines) in dBm at 2.4 GHz at the receiver module versus beam angle considering beacon signal incidence towards the RDA for the following angles: ±45°, ±30°, ±15° and 0°.

demonstrating proof of concept.

It should be mentioned that there is a noticeable side-lobe level (SLL) which is caused by the $0.85\lambda_0$ separation between the sub-arrays within the RDA transmitter. For example, at θ = -15° the measured SLL is -6 dB from the main beam maximum. This $0.85\lambda_0$ spacing is the minimum separation possible between the sub-arrays given the planar feed network layout employed to achieve CP, and this distance defines the angular range where grating lobes are not observed. In particular, the field-of-view (FOV) for the RDA can be defined by [24]: $\theta_{FOV} = \pm \arcsin\left(\frac{\lambda}{2d}\right)$ where d is the distance between each sub-array element. For the proposed RDA, the expected FOV is about ±36° and this can be observed in Fig. 8, for the ±30° incident angle cases, where the dominant side lobe increased to about 2 dB below from the steered maximum. A more compact array for the RDA and feed network implementation could reduce the SLL, but at the same time, reduce the broadside gain.

For the monostatic patterns, the flatter the curve obtained, the larger the half-power beamwidth and the better the antenna system can be at tracking with minimal power level deviations from the observed maximum. In Fig. 9, after a certain angle, the maximum of the retrodirected bistatic beam pattern starts to have a reduction in power level, mainly due to the beam steering of the transmit array as dictated by array theory [24]. For example, from about $-40°$ to $+40°$ the monostatic curve exhibits tracking, as shown in the red dashed line in Fig. 9, with a 3 dB drop in the observed maximum at broadside.

Figure 10 also reports the measured and simulated received RF power versus distance. It is worth mentioning that simulations were completed in CST considering a phased array for broadside (using the designed simulation model of the patch array for the RDA transmitter) whilst including all the output rated amplifier power levels and losses due to the active circuit elements (see Fig. 4) and transmission line connections. The minor difference between the measured and simulated values are related to the fact that simulations were performed by applying an equal magnitude and phase distribution at each transmitter element. However, given that the measurements are in the reactive NF, the elements are not equi-phased (see Fig. 2 from [10] where similar comparisons were reported). These results are important to demonstrate that the measured RDA system is able to operate in both the NF and FF regions as well a conventional phased array.

In Table III, a comparison is made between some other relevant works and our proposed RDA system. It should also be mentioned that for [25] only the received voltage is provided (and the impedance of the load is not detailed), so we are not able to report in Table III a complete comparison between [9], [10], [25], and [26]. Regardless, by studying the ranges and power values in Table III, it is clear that our proposed RDA has the highest level of received RF and DC rectified power when compared to all other works found in the literature. For example, received power levels are well above 27 dBm (which relate to a DC converted value of more than 350 mW) while 13 dBm was reported in [9] being rectified to 10 mW DC.

To provide a more relevant comparison of our proposed antenna system with other works reported in the literature, which have less antenna elements, two relevant cases of the proposed RDA have also been included in Table III. For example, for the 2×2 array, similar transmit and receive power levels are achieved when compared to [9]; i.e. received RF power levels are 13 dBm and 11 dBm for [9] and our work, respectively, considering a common range of 50 cm and a 26 dBm transmit power level. It should also be highlighted that the FSPLs at 2.4 GHz are about 8.3 dB lower when compared to 915 MHz [9]. This implies that the reported 2×2 RDA (our work) is able receive similar power levels to that of [9], while also, overcoming the related FSPLs. These results are

also related to the NF focusing property of our developed RDA system when compared to other approaches, for example digital beamforming, as in [9].

In summary, our proposed RDA for WPT offers six important characteristics that differentiates it from the classical Pon 2D-RDA architecture and the other related retrodirective and antenna systems as reported in the literature:

1) *The removal of circulators.* This can reduce costs by removing these bulky and expensive RF components typically required for isolation between the receiving and transmission paths. This can make the design more planar, whilst reducing the overall costs of the antenna system. In this work, this has been done by having separate transmit and receive antenna arrays for the RDA, as done earlier in [27]. There are also other ways to avoid the use of circulators, such as using separate transmit and receive polarizations [28], [29], as done in our RDA, as well as split frequencies for CubeSat platforms [30].
2) *Employ transmit sub-arrays for the RDA*. This will reduce the number of active elements, minimizing costs because a mixer amplifier pair is only used for each sub-array, not at each radiating element as in the classic 2-D RDA as shown in Fig. 2(a). However, this approach will reduce the self-tracking capability and the NF focusing of the RDA to just one plane; i.e. the y-z ($\phi = 90°$) plane as previously described and illustrated in Fig. 2(c).
3) *Distinct receive and transmit arrays* for the RDA. In this approach, we also employ separated transmit and receive arrays at 2.4 GHz and 2.5 GHz, respectively. This separation can reduce electromagnetic coupling between the receiver array and the network of four sub-arrays which are individually realized by one-dimensional (1-D) patch arrays and with hybrid coupler feeding. However, this requires two sets of arrays instead of just one, as in [27]. Regardless, our proposed RDA is not as compact as one which uses transceivers and proper positioning of the separated transmit and receive arrays for the RDA, and the DUC, should be considered.
4) *Circularly polarization (CP)* offers the added benefit of orientation flexibility. Moreover, isolation improvement between the receive and transmit re-radiated fields is made possible by implementing orthogonal polarizations. In this case, the retrodirected beam exhibits left-hand circularly polarization (LHCP) whilst considering right-hand circular polarization (RHCP) for the receiver array. Apart from WPT [31]–[33], CP is also a well known approach for satellite communications [34]–[36].
5) *Operation in both the NF and FF* for high-power WPT. The more classic Pon-RDA was originally considered for operation in the FF zone [15]. However, the proposed RDA of this work was measured in both the reactive and radiating NF, considering the relatively high transmit powers, as well as the FF (all results not reported for brevity), defining a diverse antenna system which can function for varied spatial ranges. Regardless, the RDA system is able to retrodirect power in both the NF and the FF zones (see Fig. 8) demonstrating tracking for various applications in addition to WPT.
6) *Near Field focusing and DUC Tracking* will only occur in one plane due to the employed subarrays; i.e. 1-D making the proposed design suitable for applications where the DUC moves close to the tracking plane (see Fig. 2(c)). A comparison between such 1-D and 2-D tracking systems is shown in Fig. 3 where reduced power values of only about 5 dB are observed from broadside to $\pm 30°$. This is also related to the fact that the receiver for the RDA system is designed with a broad beam pattern so that the transmitter module can still receive the majority of the incoming fields from the DUC which are generated by the beacon signal tone.

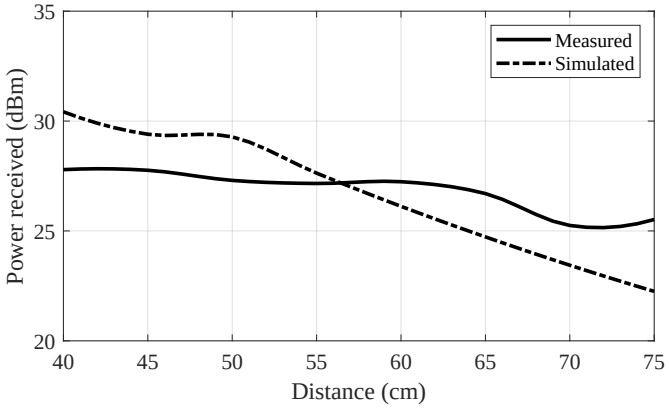

Fig. 10. Retrodirected received RF power at broadside versus distance. Given the physical size of the RDA, as well as the 2.4 GHz operating frequency, all values are defined in the reactive NF zone. It should be mentioned that the measurements were completed considering a constant beacon tone with an output power of 6.6 dBm generated by a VCO (ZX95-3000w).

IV. Conclusion

Most of the conventional systems for WPT employ inductive coupling with the main disadvantage of mobility limitations for the user. In this paper, a novel retrodirective antenna array (RDA) system for wireless power transmission which circumvents this problem was proposed. Our examined RDA employs retrodirective operation by phase conjugation of the incoming beacon signal using RF mixers. We also avoid the use of circulators by designing independent LHCP transmit and RHCP receive antenna arrays. Moreover, as the cost of more conventional RDA systems can be relatively high due to the number of amplifiers, mixers, etc. at each antenna element, we propose a hybrid solution (between a 1-D and 2-D RDA) which uses a 2-D network of linear sub-arrays that can boost the overall transmitter gain of the system.

The only challenge that this can impose is the loss of NF focusing and scanning in one plane when compared to the more conventional 2-D RDA architecture. However, results show that acceptable power levels are still observed when the DUC moves reasonably close to the desired scanning plane; i.e. reduced power values of only about 5 dB are observed over a $\pm 30°$ angular range away from the tracking plane. In general, simulations and measurements are in agreement for the RDA

TABLE III
COMPARISON OF THE PROPOSED WORK TO THE STATE-OF-THE-ART AND OTHER RELEVANT DESIGNS FOUND IN THE LITERATURE

Ref.	Freq. (MHz)	Tx Array Size ($M \times N$)	Tx Architecture	Beam tracking	Distance (m)	Field Range	Tx Power (dBm)	Rx RF Power (dBm)	Rx DC Power (mW)
[9]	915	2×2	Dig. Beamforming	Yes	0.5	NF	26	13	10
[10]	2450	16×1	RDA	Yes	1	NF	24	-	10
[25]	462.55	-	Classic Array	No	33.5	FF	36	-	3.3V
[26]	915	1×1	CP Patch	No	0.4	NF	25	-17.5	0.00514
This Work[1] (Calculated)	2400/2500	2×1	RDA	Yes	0.5	NF	33 / 26	15 / 8	23.7 / 4.7
This Work[1] (Calculated)	2400/2500	2×2	RDA	Yes	0.5	NF	33 / 26	18 / 11	47.3 / 9.4
This Work[2] (Measured) & [16]	2400/2500	4×4	RDA	Yes	0.5	NF	36	>27	>350

[1] For a fair comparison to [9], [10], [25] and [26] the proposed RDA[2] was scaled down whilst using the estimated performance values from Table I. The transmit power of 33 dBm ⟨ 26 dBm ⟩ was defined to be consistent with the proposed 4×4 RDA[2] ⟨ with [9] which operated at 915 MHz ⟩. Also, received DC power levels were calculated considering a 75% RF-to-DC rectification eficiency defining values from about 5 mW up to 50 mW.

[2] It should be mentioned that the total transmit power of 36 dBm refers to the signal strength at the output of the filters, and the power and driver amplifiers (see Fig. 4) when considering the 4 RF chains attached to the individual sub-arrays. This defines an array with 16 (= 4×4) radiating elements in total. Moreover, this power level of 30 dBm was measured by sampling the output power for the individual RF chains defined by the connected active and passive components.

and the WPT system demonstrates received power levels in excess of $27\,\mathrm{dBm}$ (and more than $350\,\mathrm{mW}$ when converted to DC using the rectifier from [16]) for a reactive NF range of $50\,\mathrm{cm}$. These results make the proposed RDA system a good alternative for mid-range WPT applications working at 2.4/2.5 GHz for operation in both the NF and FF.

REFERENCES

[1] N. Shinohara and S. Kawasaki, "Recent wireless power transmission technologies in japan for space solar power station/satellite," in *RWS 2009 IEEE Radio and Wireless Symposium, Proceedings*, San Diego, CA, 2009, pp. 13–15.

[2] N. Shinohara, "Power Without Wires," *IEEE Microwave Magazine*, vol. 12, no. 7, pp. S64–S73, 2011.

[3] B. Strassner and K. Chang, "Microwave Power Transmission: Historical Milestones and System Components," *Proceedings of the IEEE*, vol. 101, no. 6, pp. 1379–1396, 2013.

[4] J. Garnica, R. a. Chinga, and J. Lin, "Wireless power transmission: From far field to near field," *Proceedings of the IEEE*, vol. 101, no. 6, pp. 1321–1331, 2013.

[5] A. Munir and B. T. Ranum, "Wireless Power Charging System for Mobile Device Based on Magnetic Resonance Coupling," in *The 5th International Conference on Electrical Engineering and Informatics*, Bali, 2015, pp. 221–224.

[6] C.-S. Wang, O. H. Stielau, and G. A. Covic, "Design Considerations for a Contactless Electric Vehicle Battery Charger," *IEEE Transactions on Industrial Electronics*, vol. 52, no. 5, pp. 1308–1314, 2005.

[7] P. Li and R. Bashirullah, "A Wireless Power Interface for Rechargeable Battery Operated Medical Implants," *IEEE Transactions on Circuits and Systems - II: Express Briefs*, vol. 54, no. 10, pp. 912–916, 2007.

[8] P. Kildal, *Foundations of Antenna Engineering: A Unified Approach for Line-of-sight and Multipath*, ser. Artech House antennas and electromagnetics analysis library. Artech House Publishers, 2015.

[9] P. S. Yedavalli, T. Riihonen, X. Wang, and J. M. Rabaey, "Far-field rf wireless power transfer with blind adaptive beamforming for internet of things devices," *IEEE Access*, vol. 5, pp. 1743–1752, 2017.

[10] S. T. Khang, D. J. Lee, I. J. Hwang, T. D. Yeo, and J. W. Yu, "Microwave power transfer with optimal number of rectenna arrays for midrange applications," *IEEE Antennas and Wireless Propagation Letters*, vol. 17, no. 1, pp. 155–159, Jan 2018.

[11] N. Buchanan and V. Fusco, "Developments in retrodirective array technology," *IET Microwaves, Antennas & Propagation*, vol. 7, no. 2, pp. 131–140, 2013.

[12] S. L. Karode and V. F. Fusco, "Near field focusing properties of an integrated retrodirective antenna," in *IEE National Conference on Antennas and Propagation,*, April 1999, pp. 45–48.

[13] N. B. Buchanan and V. F. Fusco, "Beam steering using retrodirective array near field characteristics," in *2009 European Microwave Conference (EuMC)*, Sept 2009, pp. 1338–1340.

[14] P. D. H. Re, S. K. Podilchak, S. Rotenberg, G. Goussetis, and J. Lee, "Retrodirective antenna array for circularly polarized wireless power transmission," in *2017 11th European Conference on Antennas and Propagation (EUCAP)*, March 2017, pp. 891–895.

[15] C. Pon, "Retrodirective array using the heterodyne technique," *IEEE Transactions on Antennas and Propagation*, vol. 12, no. 2, pp. 176–180, 1964.

[16] S. A. Rotenberg, P. D. H. Re, S. K. Podilchak, G. Goussetis, and J. Lee, "An efficient rectifier for an rda wireless power transmission system operating at 2.4 ghz," in *2017 XXXIInd General Assembly and Scientific Symposium of the International Union of Radio Science (URSI GASS)*, Aug 2017, pp. 1–3.

[17] R. Y. Miyamoto and T. Itoh, "Retrodirective arrays for wireless communications," *IEEE Microwave Magazine*, vol. 3, no. 1, pp. 71–79, 2002.

[18] L. V. Atta, "Electromagnetic Reflector," Patent, 1959.

[19] S.-J. Chung, S.-M. Chen, and Y.-C. Lee, "A novel bi-directional amplifier with applications in active van atta retrodirective arrays," *IEEE Transactions on Microwave Theory and Techniques*, vol. 51, no. 2, pp. 542–547, Feb 2003.

[20] E. Rutz-Philipp, "Spherical Retrodirective Array," *IEEE Transactions on Antennas and Propagation*, vol. 12, no. 2, pp. 187–194, 1964.

[21] D. M. K. A. Yo, W. E. Forsyth, and W. A. Shiroma, "A 360 retrodirective self-oscillating mixer array," *IEEE MTT-S International*, vol. 2, pp. 813–816, 2000.

[22] G. F. Hamberger, A. Drexler, S. Trummer, U. Siart, and T. F. Eibert, "A planar dual-polarized microstrip 1d-beamforming antenna array for the 24ghz ism-band," in *2016 10th European Conference on Antennas and Propagation (EuCAP)*, April 2016, pp. 1–5.

[23] R. Garg, P. Bhartia, I. Bahl, and A. Ittipiboon, *Microstrip Antenna Design Handbook*. Artech House, 2001, ch. 8, p. 524.

[24] C. Balanis, *Antenna Theory: Analysis and Design*. Wiley, 2015.

[25] C. Cato and S. Lim, "Uhf far-field wireless power transfer for remotely powering wireless sensors," in *2014 IEEE Antennas and Propagation Society International Symposium (APSURSI)*, July 2014, pp. 1337–1338.

[26] C. Liu, Y. Zhang, and X. Liu, "Circularly polarized implantable antenna for 915 mhz ism-band far-field wireless power transmission," *IEEE Antennas and Wireless Propagation Letters*, vol. 17, no. 3, pp. 373–376, March 2018.

[27] V. F. Fusco and N. Buchanan, "Retrodirective array performance in the presence of near field obstructions," *IEEE Transactions on Antennas and Propagation*, vol. 58, no. 3, pp. 982–986, March 2010.

[28] L. Chen and S. Yan, "The design of retrodirective array in wireless sensor networks," in *2009 International Conference on Networks Security, Wireless Communications and Trusted Computing*, vol. 2, April 2009, pp. 219–222.

[29] P. Ulavapalli and M. A. Saed, "An active subharmonic retrodirective array using dual polarized microstrip antennas," in *IEEE Antennas and Propagation Society Symposium, 2004.*, vol. 4, June 2004, pp. 3939 Vol.4–.

[30] R. T. Iwami, T. F. Chun, W. G. Tonaki, and W. A. Shiroma, "A power-detecting, null-scanning, retrodirective array for a cubesat platform," in *2017 IEEE MTT-S International Microwave Symposium (IMS)*, June 2017, pp. 662–665.

[31] O. Malyuskin and V. Fusco, "Pointing accuracy and gain reduction mechanisms in cp retrodirective arrays for satcom applications," in *2012 6th European Conference on Antennas and Propagation (EUCAP)*, March 2012, pp. 825–826.
[32] O. Malyuskin, N. Buchanan, and V. Fusco, "Cp retrodirective antenna array performance degradation at large elevation angles," in *2013 7th European Conference on Antennas and Propagation (EuCAP)*, April 2013, pp. 2177–2179.
[33] L. H. Hsieh, B. H. Strassner, S. J. Kokel, C. T. Rodenbeck, M. Y. Li, K. Chang, F. E. Little, G. D. Arndt, and P. H. Ngo, "Development of a retrodirective wireless microwave power transmission system," in *IEEE Antennas and Propagation Society International Symposium. Digest. Held in conjunction with: USNC/CNC/URSI North American Radio Sci. Meeting (Cat. No.03CH37450)*, vol. 2, June 2003, pp. 393–396 vol.2.
[34] Z. Yang and K. F. Warnick, "Multiband dual-polarization high-efficiency array feed for ku/reverse-band satellite communications," *IEEE Antennas and Wireless Propagation Letters*, vol. 13, pp. 1325–1328, 2014.
[35] S. J. Sathe and J. C. Mudiganti, "A polarization reconfigurable antenna for satellite communication," in *2017 International Conference on Communication and Signal Processing (ICCSP)*, April 2017, pp. 1774–1777.
[36] O. Malyuskin, N. Buchanan, and V. Fusco, "Cp retrodirective antenna array performance degradation at large elevation angles," in *2013 7th European Conference on Antennas and Propagation (EuCAP)*, April 2013, pp. 2177–2179.

Pascual D. Hilario Re was born in Murcia, Spain. He received the B.Eng. and the M.Sc. degrees in telecommunications engineering from the Universidad Politcnica de Cartagena, Spain, in 2012 and 2015, respectively. He also received the Ph.D. degree from Heriot-Watt University, Edinburgh, Scotland, UK, in 2019. His current research interests include retrodirective systems, wireless power transmission applications, automotive radar, and analysis and design of power amplifiers.

Symon K. Podilchak (S'03–M'05) received the BASc in engineering science from the University of Toronto, ON, Canada, in 2005. While studying at Queen's University in Kingston, Ontario, Canada he received a M.A.Sc. and a Ph.D. in electrical engineering in 2008 and 2013, respectively, and he received the Outstanding Dissertation Award for his Ph.D. from the same institution. From 2013 to 2015 Symon was an Assistant Professor at Queen's. He then joined Heriot-Watt University, Edinburgh, Scotland, UK in 2015 as an Assistant Professor and became an Associate Professor in 2017. His research is also supported by a H2020 Marie Sklodowska-Curie European Research Fellowship, and, is currently a Senior Lecturer with The University of Edinburgh, School of Engineering.

He is a registered Professional Engineer (P.Eng.) and has had industrial experience as a computer programmer, and has designed 24 GHz and 77 GHz automotive radar systems with Samsung and Magna Electronics. Recent industry experience also includes the design of high frequency surface-wave radar systems, professional software design and implementation for measurements in anechoic chambers for the Canadian Department of National Defence and the SLOWPOKE Nuclear Reactor Facility. Dr. Podilchak has also designed new compact multiple-input multiple-output (MIMO) antennas for wideband military communications, highly compact circularly polarized antennas for microsatellites with COM DEV International, as well as new wireless power transmission systems for Samsung. His research interests include surface waves, leaky-wave antennas, metasurfaces, UWB antennas, phased arrays, and CMOS integrated circuits.

Dr. Podilchak and his students have been the recipient of many best paper awards and scholarships; most notably Research Fellowships from the IEEE Antennas and Propagation Society, the IEEE Microwave Theory and Techniques Society as well as the European Microwave Association. Dr. Podilchak also received a Postgraduate Fellowship from the Natural Sciences and Engineering Research Council of Canada (NSERC) and five Young Scientist Awards from the International Union of Radio Science (URSI). In 2011 and 2013 he received student paper awards at the IEEE International Symposium on Antennas and Propagation, and in 2012, the best paper prize for Antenna Design at the European Conference on Antennas and Propagation for his work on CubeSat antennas, and in 2016, received The European Microwave Prize for his research on surface waves and leaky-wave antennas. In 2017 and 2019 Dr. Podilchak was bestowed a Visiting Professorship Award at Sapienza University in Rome. In 2014, the IEEE Antennas and Propagation Society recognized Dr. Podilchak as an Outstanding Reviewer for the IEEE Transactions on Antennas and Propagation. Dr. Podilchak was also the founder and first chairman of the IEEE Antennas and Propagation Society and the IEEE Microwave Theory and Techniques Society, Joint Chapter of the IEEE Kingston Section in Canada as well as Scotland. In recognition of these services, the IEEE presented Dr. Podilchak with an Outstanding Volunteer Award in May 2015. Currently he also serves as a Lecturer for The European School of Antennas and is an Associate Editor to the journal IET Electronic Letters.

Samuel A. Rotenberg was born in Paris, France. He received an engineer diploma in Digital and Numeric Engineering System from the engineering school ENSEM in France, in 2016. He also received an M.Sc degrees in Mobile communication from the university of Heriot watt, Edinburgh, Scotland, in 2016. He received in 2017 the young scientist award at the international conference URSI GASS in Canada for his previous work. He is currently finalising his PhD in telecommunication engineering and co-founder of INFINECT, a spinout company from Heriot Watt university developing Flat Panel Antenna for Satellite Communication On the Move.

Samuel A. Rotenberg (S'99–M'02–M'12) received the Diploma degree in electrical and computer engineering from the National Technical University of Athens, Greece, in 1998, the B.Sc. degree in physics (Hons.) from University College London, U.K., in 2002, and the Ph.D. degree from the University of Westminster, London, U.K., in 2002. In 1998, he joined Space Engineering, Rome, Italy, as an RF Engineer, and as a Research Assistant with the Wireless Communications Research Group, University of Westminster, U.K., in 1999. From 2002 to 2006, he was a Senior Research Fellow with Loughborough University, U.K. He was a Lecturer (Assistant Professor) with Heriot-Watt University, Edinburgh, U.K., from 2006 to 2009, and a Reader (Associate Professor) with Queen's University Belfast, U.K., from 2009 to 2013. In 2013, he joined Heriot-Watt, as a Reader, and was promoted to Professor, in 2014.

He has authored or co-authored over 200 peer-reviewed papers five book chapters one book and two patents. His research interests include the modeling and design of microwave filters, frequency-selective surfaces and periodic structures, leaky wave antennas, microwave sensing and curing as well numerical techniques for electromagnetics. Dr. Goussetis has held a research fellowship with the Onassis Foundation in 2001, a research fellowship with the U.K. Royal Academy of Engineering from 2006 to 2011, and a European Marie-Curie experienced researcher fellowship from 2011 to 2012. He was a co-recipient of the 2011 European Space Agency Young Engineer of the Year Prize, the 2011 EuCAP Best Student Paper Prize, the 2012 EuCAP Best Antenna Theory Paper Prize, and the 2016 Bell Labs Prize.

Jaesup Lee received the M.S. degree in electrical engineering from the University of California at Los Angeles, Los Angeles, CA, USA.,He is currently with the Samsung Advanced Institute of Technology, Suwon, South Korea. His current interests include RF and analog circuits, especially ultralow-power personal network platforms and RF wireless power transfer.